EUROPEAN ORGANIZATION FOR NUCLEAR RESEARCH

August 18, 1997

Search for Scalar Leptons, Charginos and Neutralinos in e^+e^- collisions at $\sqrt{s} = 161 - 172$ GeV

The L3 Collaboration

Abstract

Searches for scalar leptons, charginos and neutralinos, predicted by supersymmetric theories, have been performed in data samples collected with the L3 detector at centre-of-mass energies of 161 GeV and 172 GeV with integrated luminosities of 10.7 pb^{-1} and 10.1 pb^{-1} respectively. No evidence for such particles is found. New limits on production cross sections are set, assuming R–parity conservation. New exclusion contours in the Minimal Supersymmetric Standard Model parameter space as well as new lower limits on masses are derived.

Submitted to *Int. Conference on High Energy Physics, Jerusalem, 1997*

1 Introduction

One of the main objectives of the LEP experiments is the search for supersymmetric particles (SUSY) predicted in theories beyond the Standard Model [1]. They are partners of the known particles with a spin difference of one half a unit. In addition supersymmetric models require at least two Higgs doublets to generate the masses of the gauge bosons and of the fermions.

In this either, following assumptions are made: R–parity, a quantum number which distinguishes ordinary particles from supersymmetric particles, is conserved and the neutralino ($\tilde{\chi}^0_1$) is the lightest supersymmetric particle. The conservation of R–parity implies that supersymmetric particles are produced in pairs and decay into non-supersymmetric particles plus the $\tilde{\chi}^0_1$ which is stable and escapes detection due to its weakly interacting nature.

Scalar leptons ($\tilde{\ell}^{\pm}_R$ and $\tilde{\ell}^{\pm}_L$) are the supersymmetric partners of the right- and left-handed charged leptons. They are produced in pairs through s-channel γ/Z exchange. The production of scalar electrons receives contributions also from the t-channel exchange of a neutralino which enhances the production cross section. The slepton decays into its associated lepton mainly via $\tilde{\ell}^{\pm} \rightarrow \tilde{\chi}^0_1 \ell^{\pm}$.

Charginos ($\tilde{\chi}^{\pm}_1$) are pair-produced via s-channel γ/Z or t-channel sneutrino ($\tilde{\nu}$) exchange. When the masses of the charged scalar leptons ($\tilde{\ell}^{\pm}$), the sneutrino and the charged Higgs bosons ($\mathrm{H}^{\pm}$) are very large ($>$ M_{W}) the $\tilde{\chi}^{\pm}_1$ decays mainly via exchange of a virtual W^*: $\tilde{\chi}^{\pm}_1 \rightarrow \tilde{\chi}^0_1 \mathrm{W}^* \rightarrow \tilde{\chi}^0_1 f \bar{f}'$. If the $\tilde{\ell}^{\pm}$ and $\tilde{\nu}$ masses are comparable to M_{W} the chargino decays via virtual slepton or sneutrino exchange and the leptonic branching ratio is enhanced. Finally for $\tilde{\ell}^{\pm}$ and $\tilde{\nu}$ lighter than the chargino, the decay modes $\tilde{\chi}^{\pm}_1 \rightarrow \tilde{\ell}^{\pm}\nu$ or $\tilde{\chi}^{\pm}_1 \rightarrow \tilde{\nu}\ell^{\pm}$ become dominant.

Neutralino pair production $\mathrm{e}^+\mathrm{e}^- \rightarrow \tilde{\chi}^0_i \tilde{\chi}^0_j$ ($i, j = 1, \ldots, 4$; ordered by their masses) proceeds via s-channel Z or t-channel scalar electron ($\tilde{\mathrm{e}}^{\pm}$) exchange. We distinguish two classes of detectable processes: $\mathrm{e}^+\mathrm{e}^- \rightarrow \tilde{\chi}^0_1 \tilde{\chi}^0_2$ and $\mathrm{e}^+\mathrm{e}^- \rightarrow \tilde{\chi}^0_2 \tilde{\chi}^0_2$. The decays of heavier neutralinos provide similar experimental signatures. When the masses of neutral SUSY Higgs bosons (h, A), the $\tilde{\ell}^{\pm}$ and the $\tilde{\nu}$ are very large, the heavier neutralinos ($\tilde{\chi}^0_j,\ j \geq 2$) decay via virtual Z^* exchange $\tilde{\chi}^0_j \rightarrow \tilde{\chi}^0_k \mathrm{Z}^* \rightarrow \tilde{\chi}^0_k f \bar{f}$ with $k < j$. For a chargino lighter than neutralinos the latter decay via virtual W^* exchange $\tilde{\chi}^0_j \rightarrow \tilde{\chi}^{\pm}_1 f \bar{f}'$ or finally via high order diagrams $\tilde{\chi}^0_j \rightarrow \tilde{\chi}^0_k \gamma$. If the $\tilde{\nu}$ and $\tilde{\ell}^{\pm}$ masses are comparable to the Z mass, the neutralino decays also via a virtual scalar lepton, enhancing the leptonic branching ratio. Finally, for $\tilde{\nu}$ and $\tilde{\ell}^{\pm}$ lighter than neutralinos the two body decays $\tilde{\chi}^0_j \rightarrow \tilde{\ell}^{\pm}\ell^{\mp}$ or $\tilde{\chi}^0_j \rightarrow \tilde{\nu}\nu$ ($\mathrm{j} \geq 2$) become dominant.

Previous limits on the existence of supersymmetric particles have been obtained by L3 [2] and other LEP experiments [3], as well as Tevatron experiments [4]. In what follows results are presented of a common search for scalar leptons, charginos and neutralinos at centre-of-mass energies of 161 and 172 GeV with the L3 experiment. Limits are presented on the production cross sections of SUSY particles and on parameters of the Minimal Supersymmetric Model (MSSM) [5]. To obtain these limits the new data are combined with our results previously obtained at lower centre-of-mass energies [2, 6, 7].

2 Data Sample and Simulation

Here we present the analysis of the data collected by the L3 detector [8] during the high energy runs of LEP in 1996, corresponding to a luminosity of 10.7 pb^{-1} at $\sqrt{s} = 161.3$ GeV, 1.0 pb^{-1} at $\sqrt{s} = 170.3$ GeV and 9.1 pb^{-1} at $\sqrt{s} = 172.3$ GeV.

Monte Carlo generators are used to simulate events from the following reactions: `PYTHIA` [9] for $\mathrm{e}^+\mathrm{e}^- \rightarrow \mathrm{q}\bar{\mathrm{q}}$, $\mathrm{e}^+\mathrm{e}^- \rightarrow \mathrm{Z}\,\mathrm{e}^+\mathrm{e}^-$ and $\mathrm{e}^+\mathrm{e}^- \rightarrow \gamma^*/\mathrm{Z}\,\gamma^*/\mathrm{Z}$; `EXCALIBUR` [10] for $\mathrm{e}^+\mathrm{e}^- \rightarrow \mathrm{W}^{\pm}\,\mathrm{e}^{\mp}\nu$;

KORALZ [11] for $e^+e^- \to \mu^+\mu^-$ and $e^+e^- \to \tau^+\tau^-$; BHAGENE3 [12] for $e^+e^- \to e^+e^-$; KORALW [13] for $e^+e^- \to W^+W^-$; have been simulated using DIAG36 [14] ($e^+e^- \to e^+e^-\ell^+\ell^-$) and PHOJET [15] ($e^+e^- \to e^+e^-$ hadrons), requiring at least 3 GeV invariant mass of the two-photon system. The number of simulated events for the background is equivalent to more than 100 times the statistics of collected data for most processes except for two-photon interactions for which it is more than three times the data statistics.

Signal events have been generated with the Monte Carlo program SUSYGEN [16], for masses of SUSY particles (M_{sp}) ranging from 45 GeV up to the kinematic limit and for ΔM

$$\Delta M = M_{sp} - M_{\tilde{\chi}_1^0}$$

values between 3 GeV and M_{sp}-1 GeV. In the case of the chargino and neutralino analyses we simulate for each decay mode at least 1000 events per $(M_{sp}, \Delta M)$ point. Moreover, for charginos, events have also been generated with the program DFGT [17], which includes the spin correlation between charginos. The signal efficiencies obtained are in agreement between the two programs.

The detector response is modelled with the GEANT [18] program which includes the effect of energy loss, multiple scattering and showering in the detector materials and in the beam pipe. By means of randomly triggered events in coincidence with the beam crossing we estimate the amount of noise in the detector. We monitor the time-dependent detector behaviour and take into account detector inefficiencies in our analyses.

Hadronic events are reconstructed using information coming from all sub-detectors. The energy of the event is obtained from the energy depositions in the electromagnetic and hadronic calorimeters and the particle momenta as measured in the central tracking and muon chambers.

An electron is identified as an electromagnetic shower matched with a track. An electromagnetic shower not matched with a track is identified as a photon. The energy measured in the electromagnetic calorimeter has to be larger than 1 GeV and is assigned to the identified electron or photon.

A muon is identified by a track in the muon chambers which is matched with a track in the central chamber. The muon momentum is required to be greater than 3 GeV.

Taus are defined as isolated hadronic narrow jets with energy larger than 2 GeV and one to three associated tracks. The energy of the tau is defined as the energy contained in a cone of 10° half opening angle around the tau direction. Its isolation is assured by requiring that there are no additional tracks and no more than two additional calorimetric clusters in a cone of 30° half opening angle and that the ratio of the energies in the two cones is less than 1.5.

Remaining clusters and tracks are classified as hadrons. Jets are reconstructed with the Durham algorithm [19] requiring the reconstruction of only two jets in order to derive an acoplanarity and an acollinearity for each event.

3 Analysis Procedure

3.1 Signal topologies and optimization procedure

As explained in the introduction we expect for all processes two undetected $\tilde{\chi}_1^0$'s in the final state. Therefore the main characteristics of supersymmetric processes under study are large missing transverse momentum, missing energy, missing mass and acoplanarity. We apply three types of criteria oriented to all possible decays of scalar leptons, charginos and neutralinos, as listed below:

- topology 1: at least two acoplanar leptons;
- topology 2: hadrons and at least one isolated lepton;
- topology 3: purely hadronic final state with high multiplicity;

To account for the three lepton types and for the different signatures of the sparticle considered in total nine different selections are performed.

The signal topologies and the associated background sources depend strongly on the mass difference between the sparticle and the lightest neutralino (ΔM), therefore all nine selections were optimized separately for three different ΔM ranges: the low ΔM range at $5-10$ GeV, the medium ΔM at $20-30$ GeV and the large ΔM at $50-60$ GeV. In the low ΔM range the expected topologies for the signal are characterized by a low multiplicity and a low visible energy. There the background is dominated by two-photon interactions. For large ΔM the signal signatures are very similar to those of W-pair production.

The selections are applied in a logical 'OR' and the combination of selections giving the maximal sensitivity is chosen according to the branching fractions of the sparticles. We take into account the overlap of the background and the signal in the different selections.

As already reported in reference [2] the cut values are *"a priori"* optimized using Monte Carlo signal and background events. The optimization procedure varies all cuts simultaneously to maximize the signal efficiency and the background rejection. In practice, we maximize the sensitivity function $1/\kappa$ which is related to the ratio between the average Poisson upper limit on the signal without background subtraction and the signal efficiency ϵ [20]

$$\kappa = \Sigma_{n=0}^{\infty} k_n P_b(n)/\epsilon$$

where k_n is the 95% confidence level Poisson upper limit and $P_b(n)$ is the Poisson distribution for n observed events with a background of b events.

3.2 Event selection

Common to all selections is the rejection of tagged two-photon interactions. We require that the sum of the energies measured in the lead-scintillator ring calorimeter and in the luminosity monitors is less than 10 GeV. These two detectors cover the polar angular range $1.5^\circ < \theta < 9^\circ$ on both sides of the interaction point.

3.2.1 Purely leptonic final states

Given the low multiplicity of the signal, events are rejected if the number of tracks is larger than 6 or if the number of calorimetric clusted (N_{cl}) is larger than 15. We then we require two or three identified leptons. The following quantities are defined: The energy depositions ($E_{25}^{\perp}$) and (E_{25}) within $\pm 25^\circ$ around the missing energy direction in the R–Φ plane (or in the space restectively), the energy deposition in a 60^0 half opening angle cone around the vector opposite to the sum of the two jet directions in space (E_{60}^{b}). When 3 leptons are identified, a cut on the sum of the three angles between the three lepton pairs (θ_{123}^{l}) is also applied. We also apply cuts on the lepton energy (E_{lep}), on the total transverse momentum of the leptons ($p_\perp$), on their maximum acollinearity and acoplanarity, on the polar angle of the missing energy vector (θ_{miss}) and on the variable E_{TTL}. The latter is defined as the absolute value of the projection of the total momentum of the two leptons onto the direction perpendicular to the leptonic thrust computed in the R-ϕ plane. The cut values optimized for the scalar lepton searches, are quoted in Table 1 for the three ΔM ranges. As an example we show in Fig. 1a) the distribution of E_{TTL} for identified purely leptonic final states. The data at $\sqrt{s} = 172$ GeV are compared to the background Monte Carlo and to the expected signal $e^+e^- \rightarrow \tilde{e}^+\tilde{e}^-$ with $M_{\tilde{e}} = 85$ GeV and $M_{\tilde{\chi}_1^0} = 30$ GeV.

3.2.2 Lepton and hadron final states

We select events with at least one isolated electron, muon or tau for which the energy, not associated to the lepton, in a cone of 30° half-opening angle around its direction is less than 2 GeV. We apply cuts on the number of tracks in the hadronic system ($N_{tk} - N_{lep}$) and the number of calorimetric clusters. Furthermore, cuts are applied on the missing energy directionon isolation (θ_{miss} and $E_{25}^{\perp}$), the total transverse momentum ($p_\perp$), on the energy of the isolated lepton (E_{lep}), on the recoil mass M_{rec}, as well as on the acoplanarity angle between the jet and the lepton and the E_{TTJL} variable; E_{TTJL} is equivalent to E_{TTL} using the momentum and the direction of the jet and the lepton. A cut on the invariant mass of the hadronic system (M_{had}) removes the WW background.

The cut values are shown in Table 2 for the three ΔM ranges. The distributions of the visible energy and of the acoplanarity are shown in Fig. 1b) and 1c) for events selected with looser cuts. The data at $\sqrt{s} = 172$ GeV are compared to background Monte Carlo and to a $e^+e^- \rightarrow \tilde{\chi}_1^+\tilde{\chi}_1^-$ signal with $M_{\tilde{\chi}_1^\pm} = 85$ GeV and $\Delta M = 50$ GeV.

3.2.3 Purely hadronic final states

The list of cuts is reported in Table 3 for the three ΔM ranges. Again, we apply cuts on N_{cl}, N_{tk}, $p_\perp$, E_{vis}, acollinearity and acoplanarity as well as on the missing energy (θ_{miss} and $E_{25}^{\perp}$). Other variables are the absolute value of the total momentum of the event along the beam line normalized to the visible energy ($p_{||}$), the recoil mass (M_{rc}) and the visible mass M_{vis}.

In the medium and large ΔM selections, a cut on the width of the two jets is applied. We define $y^\perp$ as the ratio between the scalar sum of the particle momenta transverse to the jet direction and the jet energy. This assures the selection of events with broad jets. In the low ΔM range a cut on the ratio $E_{TTJ}/p_\perp$ is applied. E_{TTJ} is equivalent to E_{TTL} using the momentum and the direction of the two jets. As an example the distribution of $p_\perp$ is shown in Figure 1d) for events selected with looser cuts. The data at $\sqrt{s} = 172$ GeV are compared to background Monte Carlo and to a $e^+e^- \rightarrow \tilde{\chi}_1^+\tilde{\chi}_1^-$ signal with $M_{\tilde{\chi}_1^\pm} = 85$ GeV and $\Delta M = 50$ GeV.

3.3 Efficiencies and background contaminations

To check the Monte Carlo background estimation we released and tightened all cuts obtained with the optimization procedure simultaneously. The number of events in data and Monte Carlo are compared at every step. As illustrated in Figures 2a) and 2b) for purely hadronic final states, data and Monte Carlo are in agreement for the medium and the large ΔM selections while in the low ΔM range the background expectation coming mainly from two-photon processes does not well reproduce the data. The vertical lines show the position of the optimized cuts. To avoid a dependence of the optimization on limited Monte Carlo statistics we use an analytical extrapolation for the background estimation (horizontal lines in Figure 2).

For a given pair of the sparticle and $\tilde{\chi}_1^0$ masses the combination of selections providing the highest sensitivity is chosen. Each candidate and background event surviving this set of selections belongs to this $M_{sparticle} - M_{\tilde{\chi}_1^0}$ combination, without imposing any additional kinematic constraint. A fraction of these results is displayed in Tables 4 to 6.

The selection efficiencies as well as the number of background events expected for a 85 or 80 GeV chargino mass for different decay channels and when assuming a 100% $W^*\tilde{\chi}_1^0$ decay mode are displayed in Table 4. In the latter case, a maximal efficiency of 55% is reached for a background contamination of 0.4 events for $\Delta M = 20$ GeV. In the low ΔM region the efficiency decreases due to the low acceptance and the two-photon interaction contamination. For large ΔM it decreases because of the WW background. To extract the total number of expected background events, we take into account the overlap between the different selections.

The selection efficiencies as well as the number of background events expected for a sum of neutralino masses $M_{\tilde{\chi}_1^0} + M_{\tilde{\chi}_2^0} = 160$ GeV and 170 GeV for different decay channels and assuming a 100% $Z^*\tilde{\chi}_1^0$ decay mode are displayed in Table 5. Compared to the chargino selection efficiencies, these efficiencies are lower due to the invisible decays of the Z^*.

The selection efficiencies at $\sqrt{s} = 172$ GeV for a 75 GeV mass scalar electron, a 65 GeV mass scalar muon or tau, as well as the background expectations, are reported for different values of ΔM in Table 6. The efficiencies vary from 30% to 62 % for scalar electrons and from 21% to 49% for scalar muons with a maximal background expectation of 0.7 event for each. In comparison, the scalar tau selection efficiencies are smaller.

Systematic errors on signal efficiencies are evaluated as for the data taken at $\sqrt{s} = 130-140$ GeV (see reference [2]). They amount to typically 5% relative, dominated by Monte Carlo statistics.

4 Results

A summary of the searches at $\sqrt{s} = 161$ and 172 GeV is given in Table 7 showing the number of candidates and expected background events. It should be noted that events can be selected by more than one selection. We do not observe any excess of data relative to what is expected from Standard Model processes.

Therefore we can set new upper limits on scalar lepton, chargino and neutralino production cross sections and new limits on the masses of these particles in the framework of the MSSM. Exclusion limits at 95% C.L. are derived following the procedure explained in reference [21]. As the background from two-photon processes is not well described by the Monte Carlo we conservatively do not include this contribution in the evaluation of the limits.

4.1 Upper limits on Scalar Lepton, Chargino and Neutralino production cross sections

To derive limits on production cross sections we use the luminosities collected at the different energies between 130 and 170 GeV without assuming a scaling of the cross section. Hence our limits correspond to luminosity weighted average cross sections.

Assuming a branching fraction of $\tilde{\ell}^\pm \rightarrow \tilde{\chi}_1^0 \ell^\pm$ equal to 100% limits are set on production cross sections for scalar electrons, muons and taus in the plane $M_{\tilde{\chi}_1^0}$ versus $M_{\tilde{\ell}^\pm}$ as depicted in Figure 3. The efficiency for the selection of scalar electrons includes the t-channel contribution. For scalar electron and muon masses below 80 GeV, and ΔM sufficiently large, cross sections above 0.55 pb and 0.38 pb can be excluded, respectively. Owing to the lower selection efficiency and the presence of a candidate event the corresponding limit for the scalar tau is 1.3 pb. Exclusions in the mass range $80 - 86$ GeV are less stringent because only data taken at $\sqrt{s} = 172$ GeV contribute.

The contours of upper limits on production cross section for the process $e^+e^- \to \tilde{\chi}_1^\pm \tilde{\chi}_1^\mp$ are shown in Figure 4 assuming $\tilde{\chi}_1^\pm \to W^* \tilde{\chi}_1^0$ for the chargino decays with standard W branching ratios (a) and for purely leptonic W decays (b). In parts of the kinematically accessible region a cross section as low as 0.5 pb is excluded for standard W branching fractions.

Similarly, cross section limits for associated neutralino production $e^+e^- \to \tilde{\chi}_1^0 \tilde{\chi}_2^0$ are derived (Figure 5) assuming only $Z^* \tilde{\chi}_1^0$ transitions in $\tilde{\chi}_2^0$ decays. For $M_{\tilde{\chi}_2^0}$ larger than ≈ 110 GeV and $\Delta M > 10$ GeV a cross section larger than 1.5 pb is ruled out.

4.2 Interpretation in the MSSM

In the MSSM, with Grand Unification assumption [22], the masses and the couplings of the gauginos and of the sparticles as well as their production cross sections are entirely described [5] once the five parameters $\tan\beta$ (the ratio of the vacuum expectation values of the two Higgs doublets), $M \equiv M_2$ (the gaugino mass parameter), μ (the higgsino mixing parameter), m_0 (the common mass for scalar fermion at the GUT scale) and A (the trilinear coupling in the Higgs sector) are fixed. The assumption of a common scalar mass scale is relevant only if light fermion partners are considered. We investigate the following MSSM parameter space:

$$\begin{array}{rcl@{\qquad}rcl} 1 \leq & \tan\beta & \leq 40 & 0 \leq & M_2 & \leq 2000 \text{ GeV} \\ -500 \text{ GeV} \leq & \mu & \leq 500 \text{ GeV} & 10 \text{ GeV} \leq & m_0 & \leq 500 \text{ GeV} \end{array}$$

The interpretation of the search results in the MSSM presented here do not depend on A.

All limits on cross section previously shown can be translated into exclusion regions in the MSSM parameter space. To derive such limits we use the generator `SUSYGEN` [16] in which cross sections and branching fractions are calculated in the MSSM framework.

4.2.1 Limits on Scalar Leptons

In general the SUSY partners of the right-handed leptons ($\tilde{\ell}_R^\pm$) are expected to be lighter than their counterparts for left-handed leptons. Hence, we show in Figure 6a) the exclusion contour in the $M_{\tilde{\chi}_1^0} - M_{\tilde{e}_R^\pm}$ plane for $\tilde{e}_R^\pm$ considering only the reaction $e^+e^- \to \tilde{e}_R^\pm \tilde{e}_R^\mp$ and for $\mu = -200$ GeV and $\tan\beta = 1.41$. To derive this exclusion only the purely leptonic decay $\tilde{e}^\pm \to e^\pm \tilde{\chi}_1^0$ is considered neglecting the efficiency for cascade decays. For $M_{\tilde{\chi}_1^0} < 48$ GeV we exclude a scalar electron lighter than 70 GeV for $\tan\beta \geq 1.41$. This significantly improves our result obtained at $\sqrt{s} = 130 - 140$ GeV [2].

With the same assumptions and considering only the reaction $e^+e^- \to \tilde{\mu}_R^\pm \tilde{\mu}_R^\mp$ we derive the lower limits on the scalar muon mass as function of $M_{\tilde{\chi}_1^0}$ shown in Figure 6b). In particular for $M_{\tilde{\chi}_1^0} < 50$ GeV we exclude a scalar muon lighter than 60 GeV independent of $\tan\beta$. This new limit improves the one obtained at the Z resonance [6].

If universality for scalar masses is assumed and combining the searches for charginos, neutralinos and scalar partners of left- and right-handed electrons and muons, lower limits on the SUSY partners of right-handed leptons as function of $M_{\tilde{\chi}_1^0}$ are obtained as shown in Figure 6c). A limit of $M_{\tilde{\ell}^\pm} \geq 73.9$ GeV is reached for $M_{\tilde{\chi}_1^0} < 47.7$ GeV. The exclusion of a light neutralino, described below, enables us to rule out $\tilde{\ell}_R^\pm$ beyond the kinematic limit of 86 GeV.

4.2.2 Limits on Chargino and Neutralino masses

In the MSSM framework, while the cross sections and couplings of the charginos and the neutralinos depend on the masses of the scalar leptons which could be exchanged in the t-channel, their masses depend only on M_2, μ and $\tan\beta$. Therefore, exclusion regions can be expressed in the $\mathrm{M}_2 - \mu$ plane for a given $\tan\beta$. The exclusions in the high m_0 range are mainly derived from chargino and neutralino searches while for low m_0 also the searches for scalar leptons contribute. Here we also take into account all chargino and neutralino cascade decays:

- $\tilde{\chi}^{\pm}_1 \rightarrow \tilde{\chi}^0_2\,\mathrm{W}^*$: We observe a slight decrease of the efficiency relative to $\tilde{\chi}^{\pm}_1 \rightarrow \tilde{\chi}^0_1\,\mathrm{W}^*$ depending on the masses of $\tilde{\chi}^0_2$, $\tilde{\chi}^{\pm}_1$ and $\tilde{\chi}^0_1$. Conservatively the lowest efficiency is used for cascade decays.

- $\tilde{\chi}^0_{3,4} \rightarrow \tilde{\chi}^0_2\,\mathrm{Z}^*$: The efficiency is found to be larger than the efficiency achieved for the $\tilde{\chi}^0_{3,4} \rightarrow \tilde{\chi}^0_1\,\mathrm{Z}^*$ channel, especially in the large ΔM region. We use conservatively the efficiencies obtained in the latter, standard channel.

Substantial extension with respect to the results obtained at $\sqrt{s} = 130 - 140$ GeV are reached as shown in Figure 7 for $\tan\beta = 1.41$ (a) and $\tan\beta = 40$. Our limits are extended by typically 20 GeV on μ and 25 GeV on M_2.

Depending on the chargino field content, one distinguishes the following cases for the derivation of lower limits on the neutralino and chargino masses:

- Higgsino-like $\tilde{\chi}^0_2$ and $\tilde{\chi}^{\pm}_1 1$ ($\mathrm{M}_2 \gg \mu$): In this case, the production cross sections do not depend on scalar lepton masses, ΔM is low and decreases with increasing M_2. Consequently the limits on the masses of the second lightest neutralino and the lightest chargino decrease with M_2 as depicted in Figures 8a) and b), respectively. For $\tan\beta = 1.41$ and M_2 less than 500 GeV, a chargino lighter than 85.0 GeV and a second lightest neutralino lighter than 92.0 GeV are excluded.

- Gaugino-like chargino ($\mu \gg \mathrm{M}_2$): The cross section depends strongly on the sneutrino mass. For 50 GeV $\leq M_{\tilde{\nu}} \leq$ 80 GeV the destructive interference term reduces the cross section by one order of magnitude compared to what is expected for $M_{\tilde{\nu}} \geq 500$ GeV. When the two body decay $\tilde{\chi}^{\pm}_1 \rightarrow \ell^{\pm}\,\tilde{\nu}$ is dominant the relevant ΔM becomes $\Delta M = M_{\tilde{\chi}^{\pm}_1} - M_{\tilde{\nu}}$. In the low ΔM region, the acceptance for charginos decreases but we benefit there from the complementary scalar lepton searches. The limits obtained in the $M_{\tilde{\chi}^{\pm}_1} - M_{\tilde{\nu}}$ plane are shown in Figure 9 for $\tan\beta = 1.41$ and two values of μ (-200 and -500 GeV). The dashed line indicates the boundary $M_{\tilde{\chi}^{\pm}_1} = M_{\tilde{\nu}}$. For small $M_{\tilde{\nu}}$ we can exclude chargino masses beyond the kinematic limit. For large $M_{\tilde{\nu}}$ and for $\mu = -500\,(200)$ GeV we obtain $M_{\tilde{\chi}^{\pm}_1} > 85.5(84.0)$ GeV which is close to the kinematic limit. Finally, for $\mu = -500\,(200)$ GeV a limit of $M_{\tilde{\chi}^{\pm}_1} > 79.8\,(69.2)$ GeV is obtained for any $M_{\tilde{\nu}}$.

We also derive limits on the mass of the lightest neutralino as shown in Figure 10a) as function of m_0. For large m_0 (≥ 200 GeV) where the limit is derived only from chargino and neutralino searches we obtain $M_{\tilde{\chi}^0_1} > 24.6$ GeV for $\tan\beta \geq 1$. For small $\tan\beta$ values and for μ values in the range –60 GeV to –70 GeV the excluded domain still benefits from the results obtained with data at the Z peak.

For low m_0 (≤ 65 GeV) the limit comes mainly from the slepton searches. In the intermediate region (65 GeV $\leq \mathrm{m}_0 \leq$ 85 GeV) the production cross section for charginos is minimal and the scalar lepton searches do not contribute anymore. In addition, heavy neutralinos ($\tilde{\chi}^0_{3,4}$)

decay mainly invisibly according to $\tilde{\chi}^0_{3,4} \rightarrow \tilde{\nu}\nu$. Therefore exclusion in this region mainly comes from radiative decays of $\tilde{\chi}^0_2$ which has been studied in reference [23]. The results shown in Figure 10 are obtained from a scan in the MSSM parameter space in steps of 1 GeV for M_2, 0.5 GeV for μ and 1 GeV for m_0. The following values of $\tan\beta$ are used: 1.0, 1.2, 1.41, 1.7, 2.0, 2.4, 3.0, 5.0 and 40.0.

In Figure 10b) we show the lower limit on $M_{\tilde{\chi}^0_1}$ as function of $\tan\beta$ for any m_0. We obtain a lower limit for the lightest neutralino of $M_{\tilde{\chi}^0_1} \geq 10.9$ GeV for $\tan\beta \geq 1$ and any value of m_0.

5 Conclusion

No evidence for SUSY particles has been found since eight candidate events survive the cuts when a number of 7.6 background events was expected. This enables us, using also data at lower energies, to set new upper limits on their production cross section. In the MSSM framework (assuming also scalar lepton mass universality and gauge mass unification) the following 95% C.L. lower limits are derived:

- $M_{\tilde{\ell}^\pm} > 73.9$ GeV for $M_{\tilde{\chi}^0_1} \leq 47.7$ GeV, $|\mu| \geq 200$ GeV and $\tan\beta \geq 1.41$;
- $M_{\tilde{\chi}^\pm_1} > 85.5$ GeV for a Gaugino-like chargino ($\mathrm{M}_{\tilde{\nu}} \geq 300$ GeV; $\mu = -500$ GeV) and $M_{\tilde{\chi}^\pm_1} > 79.8$ GeV for any $\mathrm{M}_{\tilde{\nu}}$;
- $M_{\tilde{\chi}^\pm_1} > 85.0$ GeV for a Higgsino-like chargino assuming $\mathrm{M}_2 \leq 500$ GeV and $\tan\beta = 1.41$;
- $M_{\tilde{\chi}^0_2} > 92.0$ GeV for a Higgsino-like neutralino assuming $\mathrm{M}_2 \leq 500$ GeV and $\tan\beta = 1.41$;
- $M_{\tilde{\chi}^0_1} > 24.6$ GeV for $\mathrm{m}_0 \geq 200$ GeV ($\tan\beta \geq 1$) and $M_{\tilde{\chi}^0_1} > 10.9$ GeV for any m_0 value.

These results improve significantly our previous limits.

Acknowledgements

We wish to congratulate the CERN accelerator divisions for the successful upgrade of the LEP machine and to express our gratitude for the excellent performance of the machine. We acknowledge the effort of all engineers, technicians and support staff who have participated in the construction and maintenance of this experiment.

References

[1] Y.A. Godfand and E.P. Likthman, JETP Lett.13 (1971);
D.V. Volkhov and V.P Akulov, Phys. Lett. B 46 (1973) 109;
J. Wess and B. Zumino, Nucl. Pys. B 70 (1974) 39;
P. Fayet and S. Ferrara, Phys. Rep. 32 (1977) 249;
A. Salam and J. Strathdee, Fortschr. Phys. 26 (1978)57.

[2] L3 Collab., M. Acciari et al., Phys. Lett. B 377 (1996) 289.

[3] ALEPH Collab., D. Buskulic et al., Phys. Lett. B 373 (1996) 246; Z. Phys. C 72 (1996) 549 and R. Barate et al., "Search for sleptons in e^+e^- collisions at centre-of-mass energies of 161 GeV and 172 GeV", Preprint CERN-PPE/97-56, submitted to Phys. Lett.;
DELPHI Collab., P. Abreu et al., Phys. Lett. B 387 (1996) 651 and Phys. Lett. B 382 (1996) 323;
OPAL Collaboration, K. Ackerstaff et al., Phys. Lett. B 377 (1996) 273, Phys. Lett. B 389 (1996) 616, Phys. Lett. B 396 (1997) 301, G. Alexander et al., Z. Phys. C 73 (1997) 201 and K. Ackerstaff et al., "Search for Chargino and Neutralino Production at $\sqrt{s} = 170$ and 172 GeV at LEP", Preprint CERN-PPE/97-83, submitted to Z. Phys.

[4] CDF Collab., F. Abe et al., Phys. Rev. Lett. 76 (1996) 4307;
D0 Collab., S. Abachi et al., Phys. Rev. Lett. 76 (1996) 2228.

[5] See for instance:
H.P. Nilles, Phys. Rep. 110 (1984)1;
H.E. Haber and G.L. Kane, Phys. Rep. 117 (1985) 75;
R. Barbieri, Riv. Nuovo Cim. 11 n° 4 (1988) 1.

[6] L3 Collab., O. Adriani et al., Phys. Rep. 236 (1993) 1.

[7] L3 Collab., M. Acciarri et al., Phys. Lett. B 350 (1995) 109.

[8] L3 Collab., B. Adeva et al., Nucl. Instr. and Meth. A 289 (1990) 35;
M. Chemarin et al., Nucl. Instr. and Meth. A 349 (1994) 345; M. Acciari et al., Nucl. Instr. and Meth. A 351 (1994) 300; G. Basti et al., Nucl. Instr. and Meth. A 374 (1996) 293; I. Brock et al., Nucl. Instr. and Meth. A 381 (1996) 236; A. Adam et al., Nucl. Instr. and Meth. A 383 (1996) 342.

[9] T. Sjöstrand, `PYTHIA 5.7` and `JETSET 7.4` Physics and Manual, CERN–TH/7112/93 (1993), revised August 1995; Comp. Phys. Comm. 82 (1994) 74.

[10] F.A. Berends, R. Kleiss and R. Pittau, Nucl. Phys. B 424 (1994) 308; Nucl. Phys. B 426 (1994) 344; Nucl. Phys. (Proc. Suppl.) B 37 (1994) 163; Phys. Lett. B 335 (1994) 490; Comp. Phys. Comm. 83 (1994) 141.

[11] `KORALZ` version 4.01 is used.
S. Jadach, B.F.L. Ward and Z. Wąs, Comp. Phys. Comm. 79 (1994) 503.

[12] `BHAGENE` version 3 is used.
J.H. Field, Phys. Lett. B 323 (1994) 432;
J.H. Field and T. Riemann, Comp. Phys. Comm. 94 (1996) 53.

[13] KORALW version 1.21 is used.
M. Skrzypek, S. Jadach, W. Placzek and Z. Wąs, Comp. Phys. Comm. 94 (1996) 216;
M. Skrzypek, S. Jadach, M. Martinez, W. Placzek and Z. Wąs, Phys. Lett. B 372 (1996) 289.

[14] F.A. Berends, P.H. Daverfeldt and R. Kleiss, Nucl. Phys. B 253 (1985) 441.

[15] PHOJET version 1.05 is used.
R. Engel, Z. Phys. C 66 (1995) 203;
R. Engel and J. Ranft, Phys. Rev. D 54 (1996) 4244.

[16] The SUSYGEN generator, S. Katsanavas and M. Melachroinos, Proceedings of the Workshop "Physics at LEP2", Report CERN 96-01 (1996), eds. G. Altarelli, T. Sjöstrand, F. Zwirner, Vol.2, p. 328.

[17] The DFGT generator, C. Dionisi et al., Proceedings of the Workshop "Physics at LEP2", Report CERN 96-01 (1996), eds. G. Altarelli, T. Sjöstrand, F. Zwirner, Vol.2, p. 337.

[18] The L3 detector simulation is based on GEANT Version 3.15. See R. Brun et al., "GEANT3", CERN DD/EE/84-1 (Revised), September 1987;
The GHEISHA program (H. Fesefeldt, RWTH Aachen Report PITHA 85/02 (1985)) is used to simulate hadronic interactions.

[19] S. Catani et al., Phys. Lett. B 269 (1991) 432;
S. Bethke et al., Nucl. Phys. B370 (1992) 310.

[20] J.F Grivaz, F. Le Diberder, preprint LAL-92-37, June 1992.

[21] R.D. Cousins and V.L. Highland, Nucl. Instr. and Meth. A 320 (1992) 331.

[22] See for instance:
L. Ibanez, Phys. Lett. B 118 (1982) 73;
R. Barbieri, S. Farrara, C. Savoy, Phys. Lett. B 119 (1982) 343.

[23] L3 Collab., M. Acciarri et al., "Single and Multi-Photon Events with Missing Energy in e^+e^- Collisions at 161 GeV $< \sqrt{s} <$ 172 GeV", Preprint CERN-PPE/97-76; submitted to Phys. Lett.

scalar electron selection				
		Low ΔM	Medium ΔM	High ΔM
E_{lep} (GeV)	$\leq$	23.7	43.6	67
E_{lep} (GeV)	$\geq$	2.63	19.7	14
E_{lep}/E_{vis} (GeV)	$\leq$	0.34	0.39	0.7
$p_{\perp}$ (GeV)	$\geq$	2.1	5.4	11
Acollinearity (rad)	$\leq$	2.0	2.6	3.13
Acoplanarity (rad)	$\leq$	3.1	3.0	3.0
$E_{25}^{\perp}$ (GeV)	$\leq$	–	1.8	4.4
E_{25} (GeV)	$\leq$	–	4.5	2.2
E_{60}^{b} (GeV)	$\leq$	5.5	5.4	3.1
$\sin(\theta_{miss})$	$\geq$	0.3	0.3	0.39
E_{TTL} (GeV)	$\geq$	2.5	4.9	4.9
scalar muon selection				
E_{lep} (GeV)	$\leq$	24	39	73
E_{lep} (GeV)	$\geq$	2.1	19.7	10.6
E_{lep}/E_{vis} (GeV)	$\leq$	0.34	0.48	0.7
$p_{\perp}$ (GeV)	$\geq$	2.1	5.4	11
Acollinearity (rad)	$\leq$	3.1	3.0	3.1
Acoplanarity (rad)	$\leq$	3.1	3.0	3.0
$E_{25}^{\perp}$ (GeV)	$\leq$	–	6.3	6.5
E_{25} (GeV)	$\leq$	0.7	7.2	1.6
E_{60}^{b} (GeV)	$\leq$	9.6	3.3	4.9
$\sin(\theta_{miss})$	$\geq$	0.3	0.3	0.3
E_{TTL} (GeV)	$\geq$	1.1	2.1	3.6
scalar tau selection				
E_{lep} (GeV)	$\leq$	19	26	29
E_{lep} (GeV)	$\geq$	2.1	10.6	15.
E_{lep}/E_{vis} (GeV)	$\leq$	0.19	0.36	0.41
$p_{\perp}$ (GeV)	$\geq$	2.9	5.3	10.7
Acollinearity (rad)	$\leq$	3.1	2.7	2.5
Acoplanarity (rad)	$\leq$	3.0	3.0	2.5
$E_{25}^{\perp}$ (GeV)	$\leq$	–	1.7	1.8
θ_{123}^{l} (rad)	$\leq$	–	5.1	4.3
E_{60}^{b} (GeV)	$\leq$	–	2.9	3.3
$\sin(\theta_{miss})$	$\geq$	0.66	0.6	–
E_{TTL} (GeV)	$\geq$	2.1	4.8	2.5

Table 1: Values of the cuts optimized for the scalar lepton searches and for various ΔM ranges. They have been determined with the optimization procedure described in section 3.1

Inclusive lepton plus hadrons selections				
		Low ΔM	Medium ΔM	High ΔM
N. of isolated lepton	$\geq$	1	1	1
N_{tk} -N_{lep}	$\geq$	2	4	4
N_{cl}	$\geq$	6	10	10
$\sin(\theta_{miss})$	$\geq$	0.55	0.38	0.36
$E_{25}^{\perp}$ (GeV)	$\leq$	6.9	–	7.9
$p_{\perp}$ (GeV)	$\geq$	5.5	3.2	4.7
E_{lep} (GeV)	$\geq$	1.8	4.2	7.5
E_{lep} (GeV)	$\leq$	12.4	42.6	38
E_{TTJL} (GeV)	$\geq$	0.8	–	–
Acoplanarity (rad)	$\leq$	–	2.97	3.04
M_{had} (GeV)	$\leq$	–	34	46.3
M_{rec} (GeV)	$\geq$	137	81.5	56
E_{vis} (GeV)	$\geq$	4	5	5
E_{vis} (GeV)	$\leq$	23.7	114	90

Table 2: Values of the cuts for the lepton plus hadrons selections; they have been determined with the optimization procedure described in section 3.1.

Purely hadronic selection				
		Low ΔM	Medium ΔM	High ΔM
$p_{\perp}$ (GeV)	$\geq$	6.8	7.9	23.7
$p_{\perp}/E_{vis}$	$\geq$	–	0.24	0.29
E_{vis} (GeV)	$\leq$	29.3	63.6	96.6
Acollinearity (rad)	$\leq$	2.7	2.7	2.0
Acoplanarity (rad)	$\leq$	3.1	2.5	2.9
$\sin(\theta_{miss})$	$\geq$	0.46	0.2	0.59
$E_{25}^{\perp}$ (GeV)	$\leq$	0.5	9.2	7.44
E_{25} (GeV)	$\leq$	–	–	4.82
$p_{\parallel}$	$\leq$	0.65	0.70	0.53
M_{vis} (Gev)	$\geq$	1.1	15.7	–
M_{rec} (Gev)	$\geq$	–	103	36.5
$E_{vis}/\sqrt{(s)}$	$\geq$	–	–	0.36
$E_{TTJ}/p_{\perp}$	$\geq$	0.24	–	–
$y^{\perp}$	$\geq$	–	0.23	0.28

Table 3: Values of the cuts for the purely hadronic selection ; they have been determined with the optimization procedure described in section 3.1.

$M_{\tilde{\chi}_1^\pm} = 80$ GeV					$\sqrt{s}$=161 GeV			
	LH		LL		HH		$\tilde{\chi}_1^0\,\mathrm{W}^*$	
ΔM(GeV)	ϵ (%)	N_{exp}	ϵ (%)	N_{exp}	ϵ (%)	N_{exp}	ϵ (%)	N_{exp}
5	4.4	0.5	1.7	0.3	5.3	0.2	4.3	0.6
10	44	0.3	34	0.3	40	0.4	30	0.3
20	58	0.1	48	0.2	64	0.2	50	0.3
30	57	0.1	53	0.2	48	0.5	45	0.6
40	68	0.3	50	0.1	39	0.6	44	0.8
60	54	0.5	40	0.3	16	0.1	31	0.8
75	26	0.5	20	0.3	3	0.1	18	1.0
$M_{\tilde{\chi}_1^\pm} = 85$ GeV					$\sqrt{s} = 172$ GeV			
	LH		LL		HH		$\tilde{\chi}_1^0\,\mathrm{W}^*$	
ΔM(GeV)	ϵ (%)	N_{exp}	ϵ (%)	N_{exp}	ϵ (%)	N_{exp}	ϵ (%)	N_{exp}
5	4.7	0.5	12	0.4	4.3	0.3	4.4	0.8
10	40	0.3	33	0.4	37	0.3	29	0.3
20	65	0.2	44.	0.2	66	0.2	55	0.3
30	73	0.2	57	0.3	60	0.3	52	0.3
40	70	0.3	58	0.6	30	0.9	42	1.1
60	62	0.7	27	0.6	23	0.2	30	0.6
75	27	0.5	20	0.5	5	0.2	18	1.1

Table 4: Chargino efficiencies (ϵ) for the lepton plus hadrons (LH), the purely leptonic (LL) and the purely hadronic final state (HH) and if assuming 100% $\tilde{\chi}_1^0\,\mathrm{W}^*$ decay mode. N_{exp} is the number of events expected from the standard processes. Results are given as a function of $\Delta M = M_{\tilde{\chi}_1^\pm} - M_{\tilde{\chi}_1^0}$ for $M_{\tilde{\chi}_1^\pm} = 80(85)$ GeV pair production at 161(172) GeV.

$M_{\tilde{\chi}_1^0} + M_{\tilde{\chi}_2^0} = 160$ GeV	$\sqrt{s} = 161$ GeV					
	HH		LL		$\tilde{\chi}_1^0$ Z*	
ΔM(GeV)	ϵ (%)	N_{exp}	ϵ (%)	N_{exp}	ϵ (%)	N_{exp}
10	13	0.5	7.2	0.4	10	0.5
20	37	0.3	12	0.5	24	0.2
30	42	0.4	12	0.1	31	0.5
40	48	0.3	36	0.3	35	0.4
50	57	0.3	17	0.3	41	0.5
70	36	0.8	18	0.4	26	0.8
80	22	0.8	28	1.	17	0.8
120	3	0.6	10	0.9	3	1.4
$M_{\tilde{\chi}_1^0} + M_{\tilde{\chi}_2^0} = 170$ GeV	$\sqrt{s} = 172$ GeV					
	HH		LL		$\tilde{\chi}_1^0$ Z*	
ΔM(GeV)	ϵ (%)	N_{exp}	ϵ (%)	N_{exp}	ϵ (%)	N_{exp}
10	14	0.5	32	0.4	13	0.6
20	52	0.4	42	0.5	40	0.5
30	46	0.4	40	0.4	35	0.5
40	39	0.4	39	0.4	32	0.7
50	24	0.3	35	0.3	20.	0.6
70	50	0.7	35	1.8	37	0.8
90	26	0.5	35	1.8	18	0.5
130	3	0.5	33	2.3	6	2.4

Table 5: Neutralino efficiencies (ϵ) for the purely hadronic (HH) and the purely leptonic final state (LL) and if assuming 100% $\tilde{\chi}_1^0$ Z* decay mode. N_{exp} is the number of events expected from the standard processes. Results are given as a function of $\Delta M = M_{\tilde{\chi}_2^0} - M_{\tilde{\chi}_1^0}$ for $M_{\tilde{\chi}_2^0} + M_{\tilde{\chi}_1^0} =$ 160(170) GeV at 161(172) GeV.

	$\sqrt{s} = 161$ GeV					
	$M_{\tilde{e}^\pm} = 70$ GeV		$M_{\tilde{\mu}^\pm} = 60$ GeV		$M_{\tilde{\tau}^\pm} = 50$ GeV	
	$\tilde{e}^\pm\tilde{e}^\mp$		$\tilde{\mu}^\pm\tilde{\mu}^\mp$		$\tilde{\tau}^\pm\tilde{\tau}^\mp$	
ΔM(GeV)	ϵ (%)	N_{exp}	ϵ (%)	N_{exp}	ϵ (%)	N_{exp}
5	31	0.03	24	0.2	3.5	0.3
10	51	0.1	40	0.1	12	0.4
20	60	0.1	41	0.1	17	0.7
30	62	0.4	47	0.3	15	0.5
40	61	0.4	46	0.3	15	0.5
45	61	0.4	49	0.3	15	0.5
55	58	0.4	45	0.3	–	–
65	47	0.4	–	–	–	–
	$\sqrt{s} = 172$ GeV					
	$M_{\tilde{e}^\pm} = 75$ GeV		$M_{\tilde{\mu}^\pm} = 65$ GeV		$M_{\tilde{\tau}^\pm} = 55$ GeV	
	$\tilde{e}^\pm\tilde{e}^\mp$		$\tilde{\mu}^\pm\tilde{\mu}^\mp$		$\tilde{\tau}^\pm\tilde{\tau}^\mp$	
ΔM(GeV)	ϵ (%)	N_{exp}	ϵ (%)	N_{exp}	ϵ (%)	N_{exp}
5	30	0.03	21	0.1	3.3	0.3
10	50	0.2	41	0.1	12	0.4
20	60	0.2	47	0.1	18	0.7
30	53	0.1	47	0.3	18	0.5
40	61	0.7	47	0.3	18	0.5
50	56	0.7	49	0.3	16	0.5
60	59	0.7	45	0.3	–	–
70	50	0.7	–	–	–	–

Table 6: scalar electron, scalar muon and scalar tau efficiencies (ϵ) and the number of events expected from the standard processes (N_{exp}). Results are obtained at 161 and 172 GeV for different values of $M_{\tilde{\ell}^\pm}$ as a function of $\Delta M = M_{\tilde{\ell}^\pm} - M_{\tilde{\chi}_1^0}$.

	N_{data}	N_{exp}
$\tilde{\chi}_1^\pm$, $\tilde{\chi}_1^0$	5	4.5
$\tilde{e}^\pm$	3	1.3
$\tilde{\mu}^\pm$	0	1.3
$\tilde{\tau}^\pm$	1	1.2
Overall	8	7.6

Table 7: Results on chargino, neutralino and scalar leptons searches: N_{exp} is the number of expected events from standard processes and N_{data} is the number of observed data, for the total integrated luminosity recorded at 161 and 172 GeV.

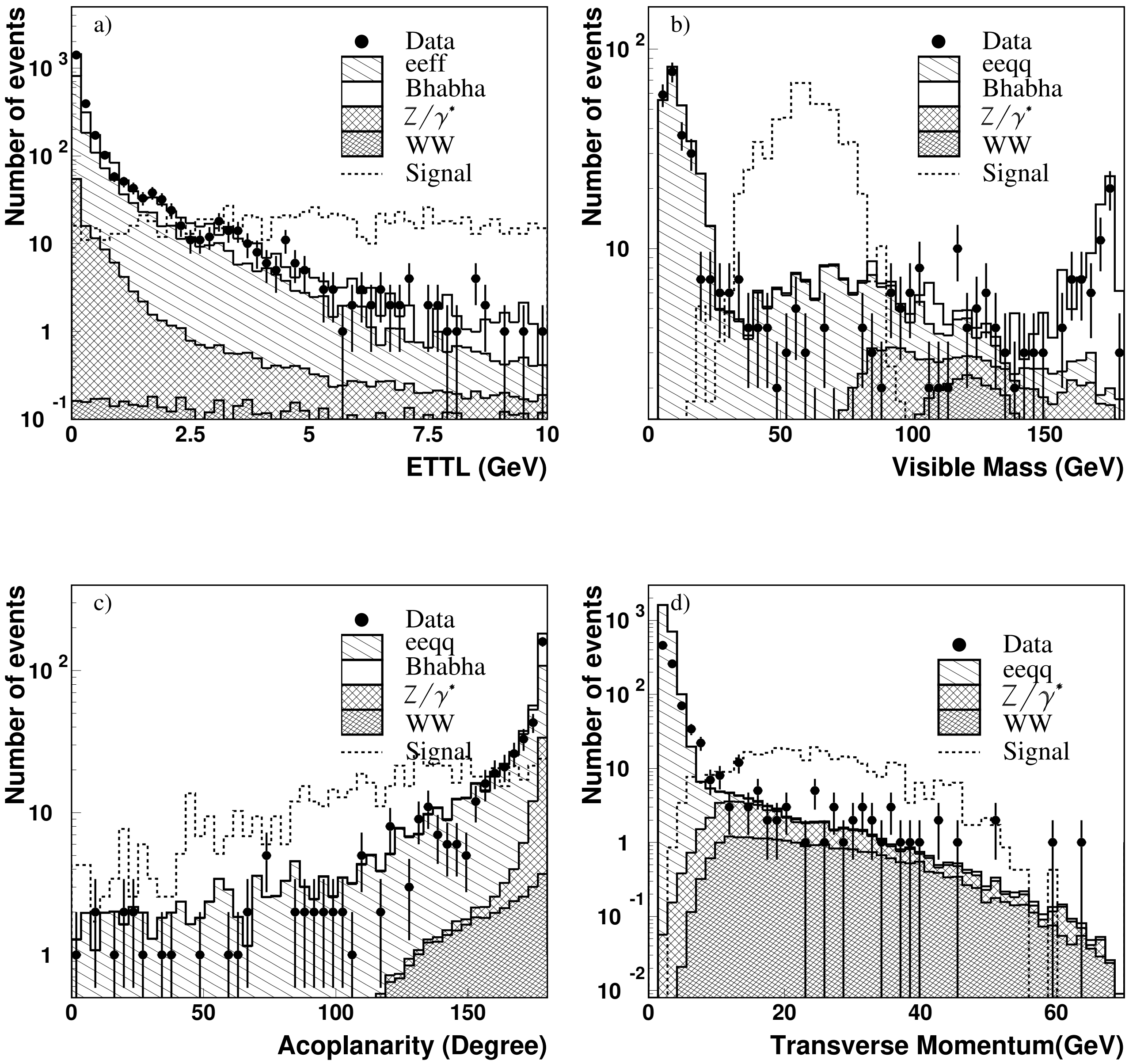

Figure 1: Distributions illustrating the selection of signal events at $\sqrt{s} = 172$ GeV. Data are compared to Standard Model background processes (hatched histograms) and to the expected signal (open histograms): a) The variable E_{TTL} (see section 3.2.1) for purely leptonic final states. b) Visible energy and c) acoplanarity of lepton plus hadrons final states. d) The distribution of the transverse momentum in purely hadronic final states. The signal distributions are evaluated for $M_{\tilde{\chi}_1^\pm} = 85$ GeV and $M_{\tilde{\chi}_1^0} = 30$ GeV for a) and $M_{\tilde{\chi}_1^0} = 50$ GeV for b)–d).

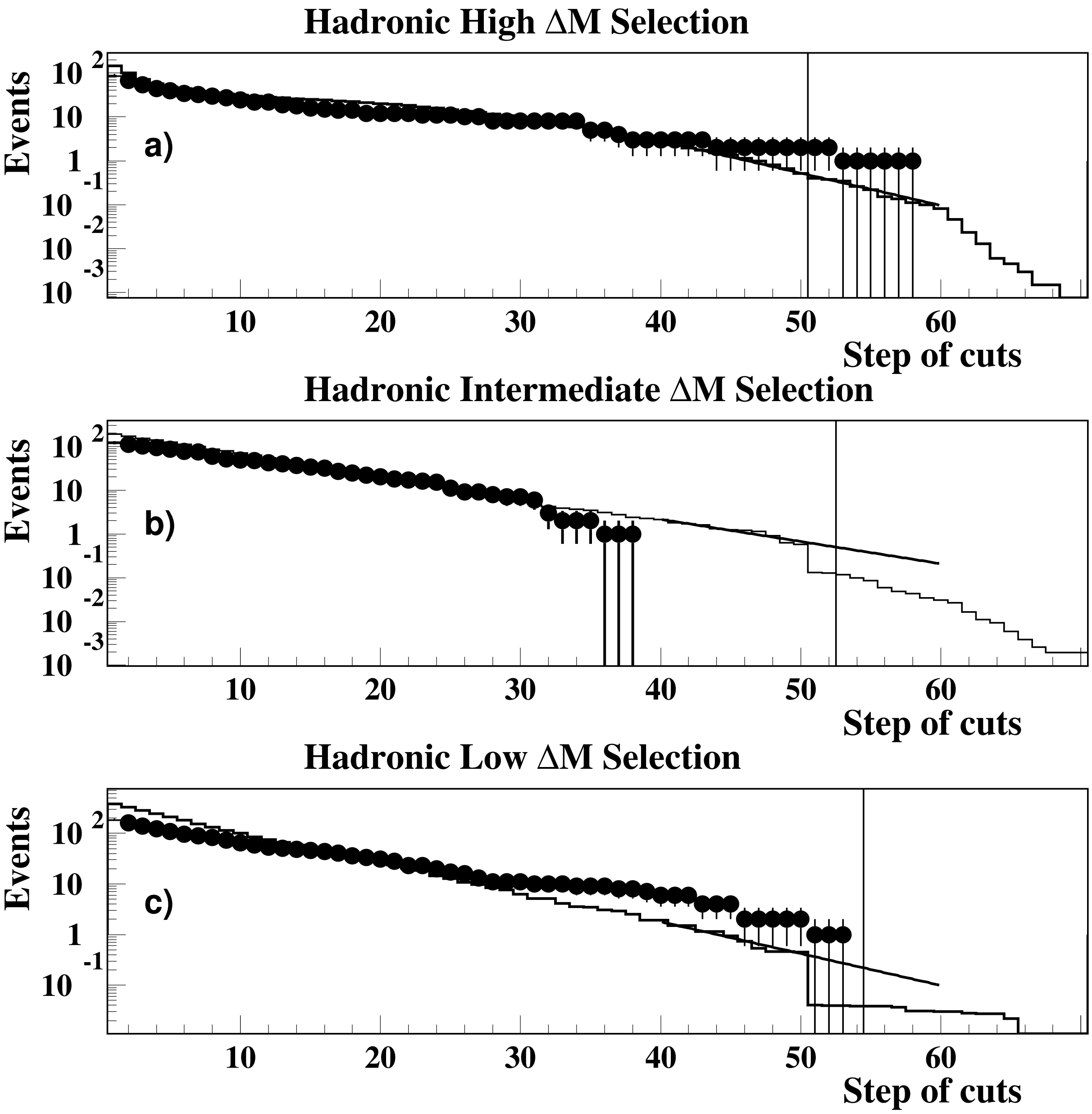

Figure 2: Number of events selected in data and in Monte Carlo simulations of Standard Model processes as function of selection cuts with increasing background rejection. the vertical lines show the position of the optimazed cuts; The superimposed lines corresponds to the analytical extrapolation for the background estimation. a), b) and c) show the distributions for the high, medium and low ΔM selection of purely hadronic final states, respectively.

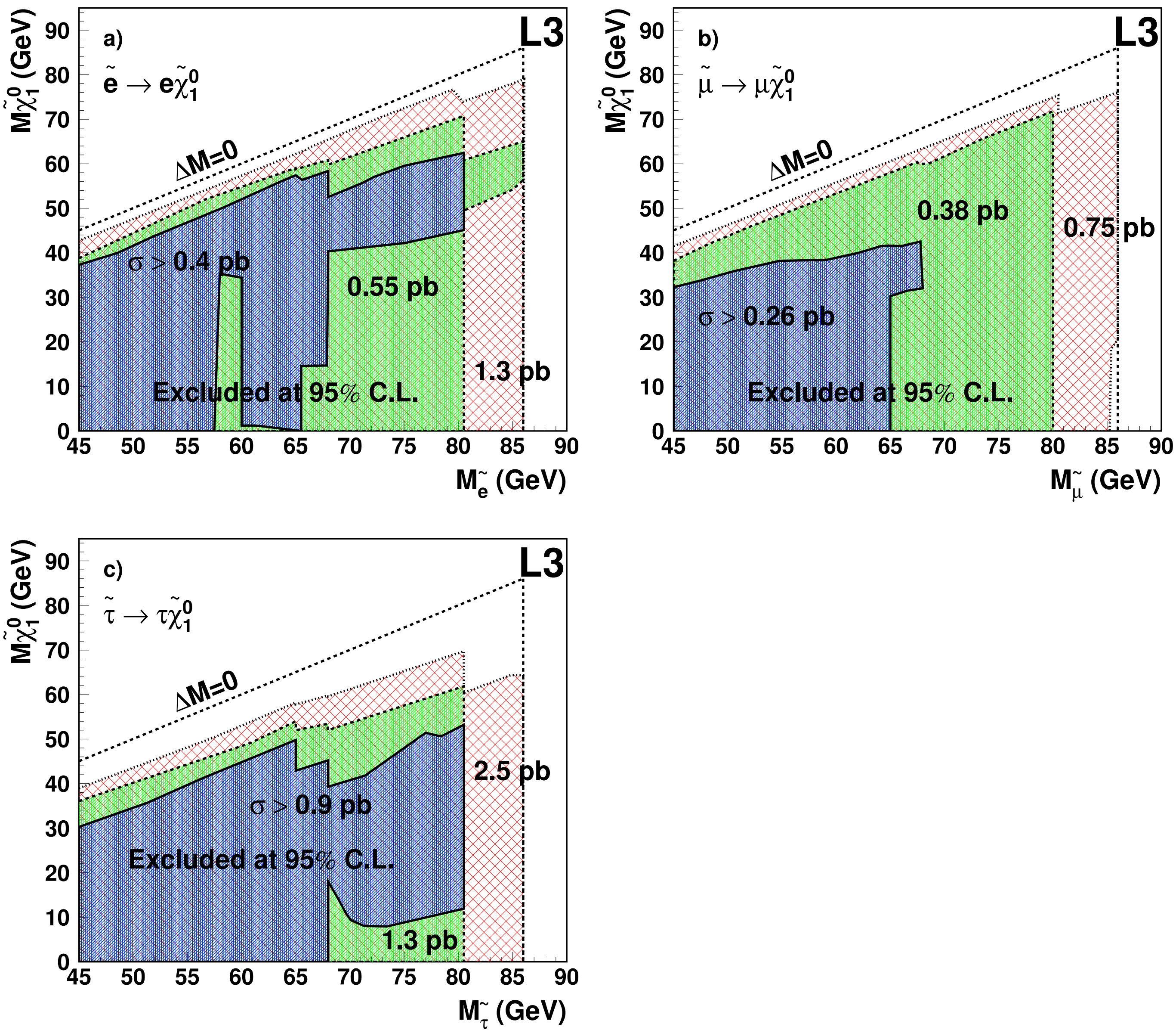

Figure 3: Upper limits on the production cross sections (in pb) for scalar leptons as function of the lightest neutralino mass $M_{\tilde{\chi}^0_1}$. a) – c) show the limits for scalar electrons, muons and taus, respectively.

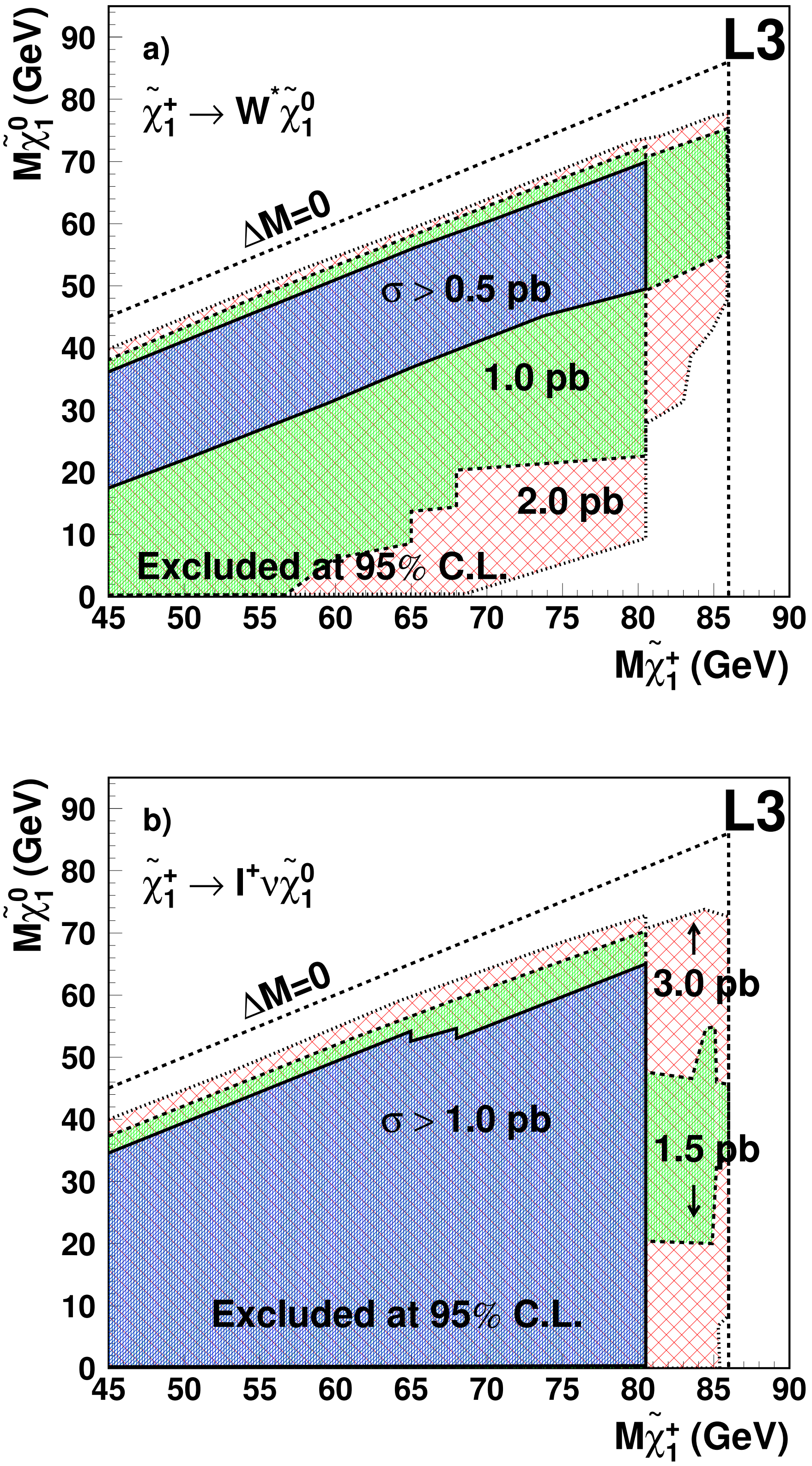

Figure 4: Upper limits on the production cross section $e^+e^- \rightarrow \tilde{\chi}_1^+\tilde{\chi}_1^-$ in the $M_{\tilde{\chi}_1^0} - M_{\tilde{\chi}_1^\pm}$ plane. a) Exclusion limits are obtained assuming standard W branching ratios in the chargino decay $\tilde{\chi}_1^\pm \rightarrow W^{*\pm}\tilde{\chi}_1^0$ and b) assuming purely leptonic W decays $(\tilde{\chi}_1^\pm \rightarrow \ell^\pm \nu \tilde{\chi}_1^0, (\ell = e, \mu, \tau))$

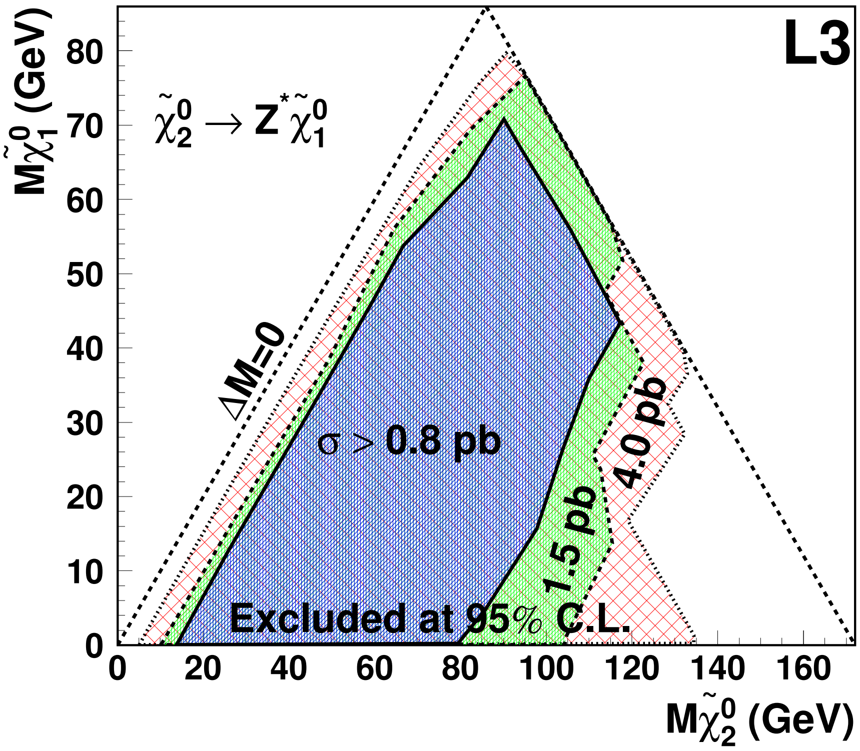

Figure 5: Upper limit on the production cross section of $e^+e^- \rightarrow \tilde{\chi}^0_1\tilde{\chi}^0_2$ in the $M_{\tilde{\chi}^0_1} - M_{\tilde{\chi}^0_2}$ plane.

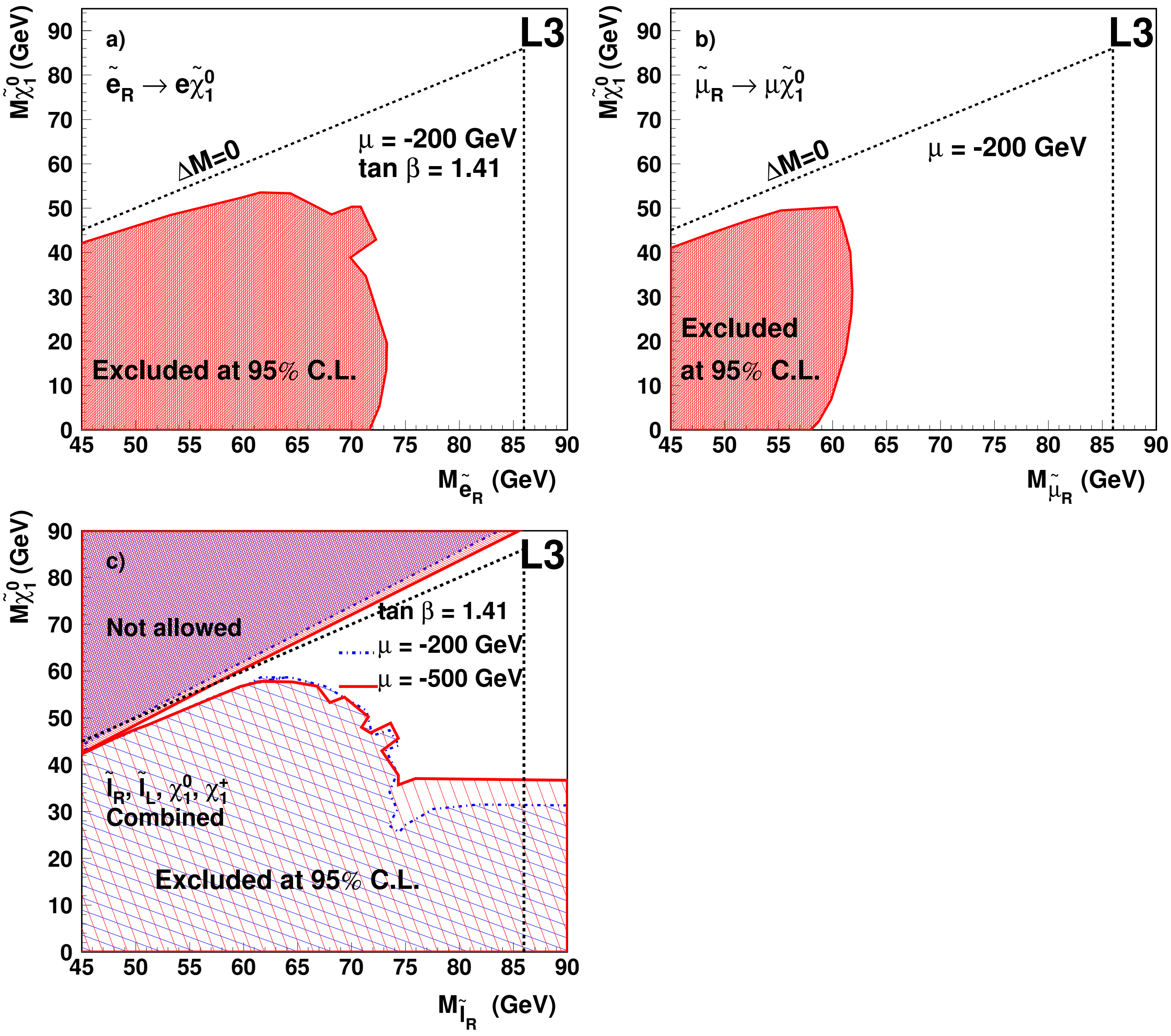

Figure 6: Mass limits on the scalar partners of right handed electrons (a) and muons (b) as function of the neutralino mass $M_{\tilde{\chi}^0_1}$. These two figures are obtained using only the upper cross section limits from the direct searches. c) shows the limits for scalar leptons assuming universality for scalar masses. This curve is derived from the search results for scalar leptons, charginos and neutralinos in the constrained MSSM.

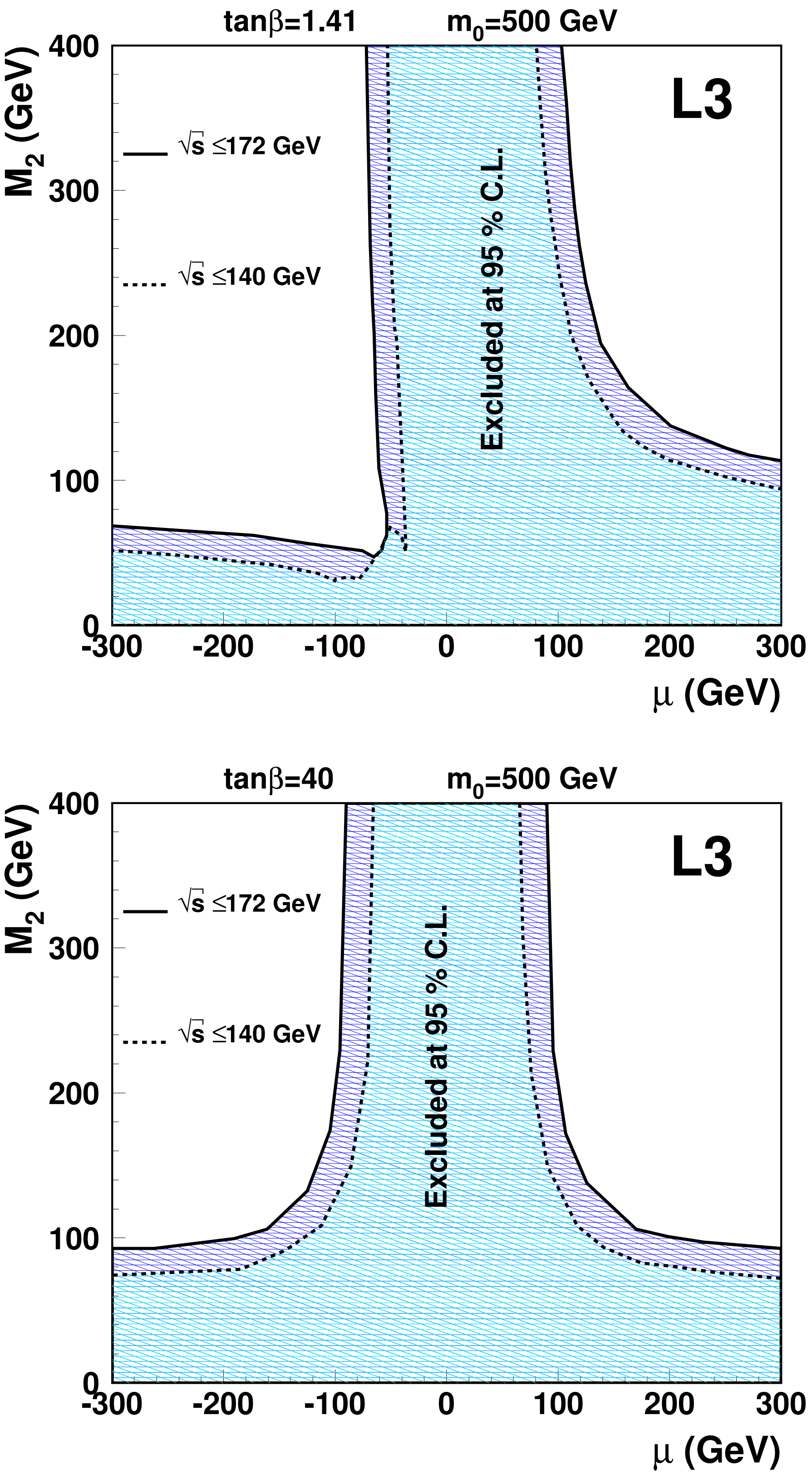

Figure 7: Exclusion regions in the M_2-μ plane derived from the search for charginos and neutralinos for $m_0 = 500$ GeV with $\tan\beta = 1.14$ (a) and 40 (b). The results using all data (solid lines) are compared to the limits obtained using only data collected at the Z resonance and at 130-140 GeV (broken lines).

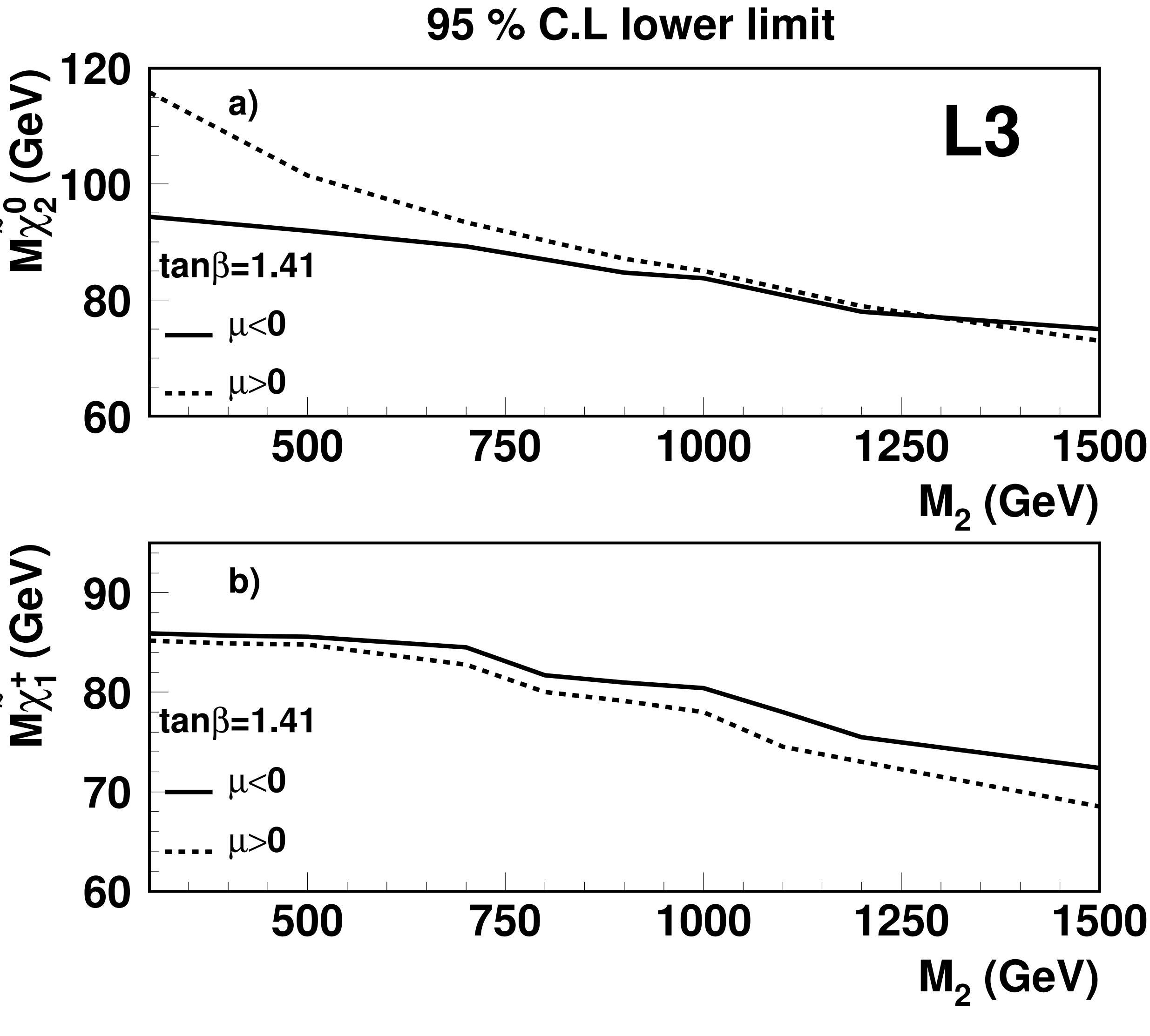

Figure 8: Mass limits as function of M_2 for the second lightest neutralino $\tilde{\chi}_2^0$ (a) and the lightest chargino $\tilde{\chi}_1^\pm$ (b). The limits are obtained for $\tan\beta = 1.41$ and for $\mu < 0$ and $\mu > 0$ (solid and broken lines, respectively).

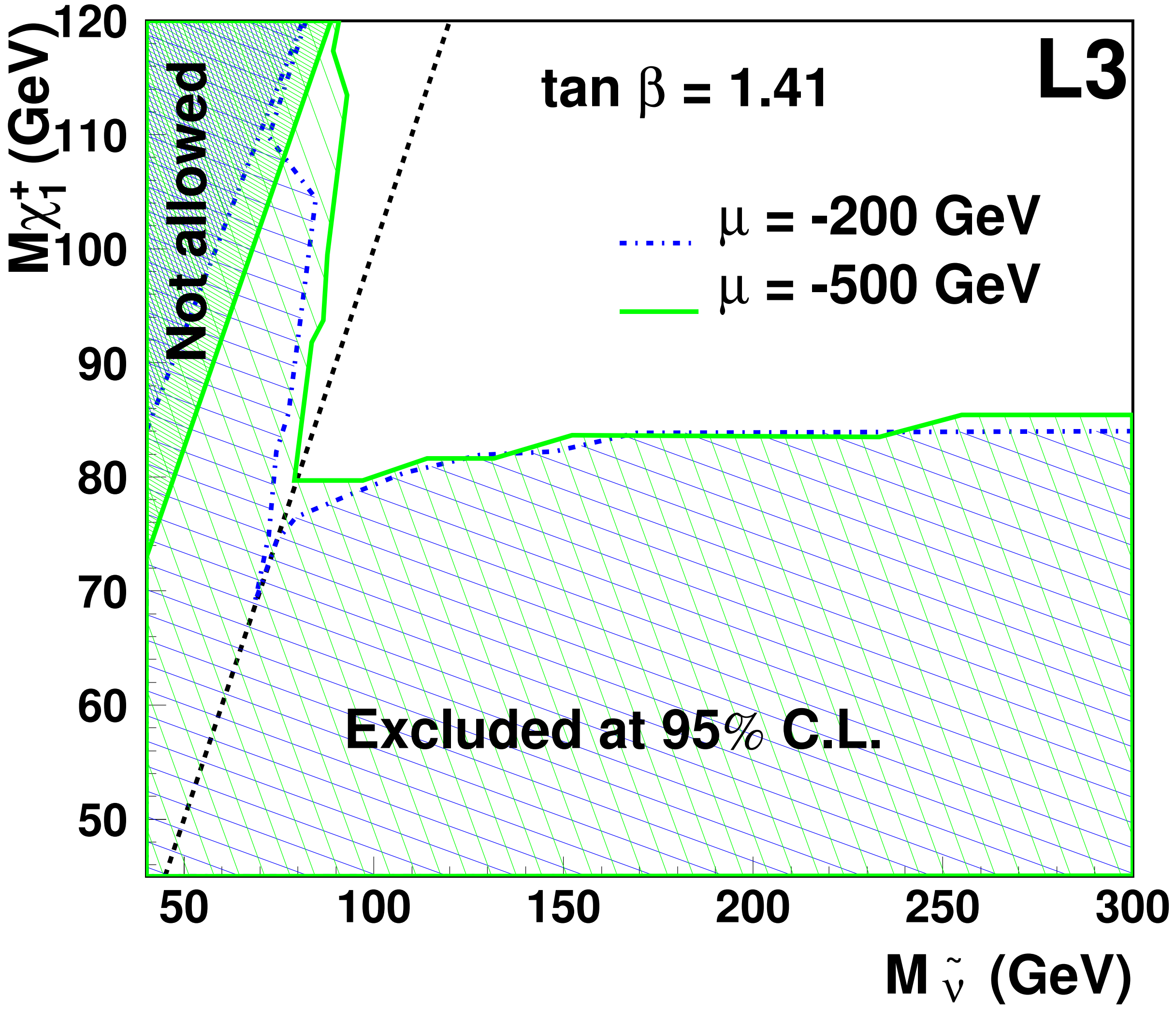

Figure 9: Mass limit for the chargino as function of the sneutrino mass for $\mu = -500$ GeV (solid line) and $\mu = -200$ GeV (broken line) for $\tan\beta = 1.41$.

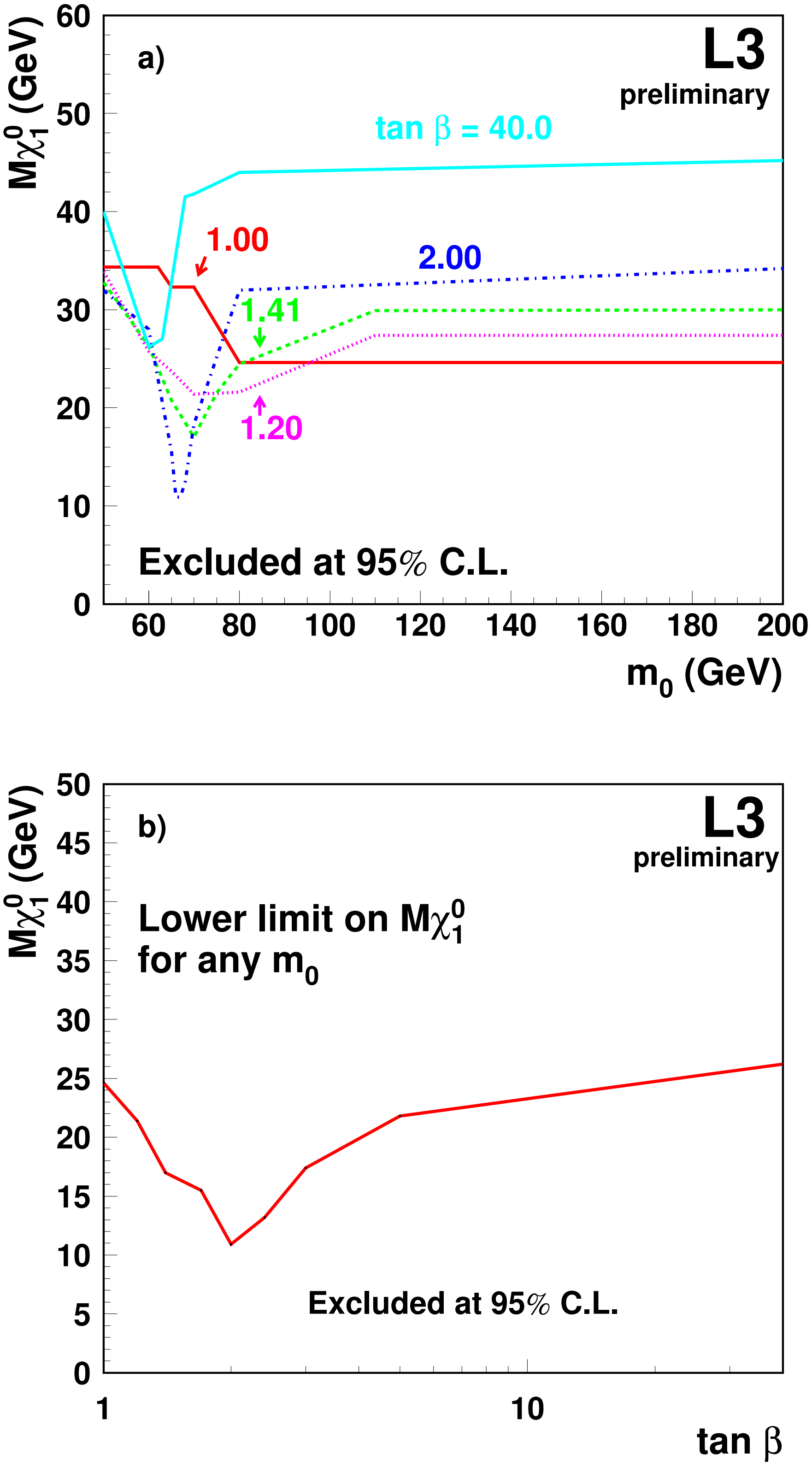

Figure 10: a) Lower limit on the neutralino mass $M_{\tilde{\chi}_1^0}$ as function of m_0 for four different values of $\tan\beta$. b) Lower limit on $M_{\tilde{\chi}_1^0}$ as function of $\tan\beta$ and for any value of m_0.